

# Fast Indirect Illumination Using Two Virtual Spherical Gaussians (Supplemental Material)

Yusuke Tokuyoshi \*  
Square Enix Co., Ltd.

## 1 Spherical Gaussians

A spherical Gaussian (SG) is a type of spherical function and is represented by using a Gaussian function  $g$  as follows:

$$G(\boldsymbol{\omega}, \boldsymbol{\xi}, \lambda) = g\left(\|\boldsymbol{\omega} - \boldsymbol{\xi}\|, \frac{1}{\lambda}\right) = e^{\lambda((\boldsymbol{\omega} \cdot \boldsymbol{\xi}) - 1)},$$

where  $\boldsymbol{\xi}$  is the lobe axis, and  $\lambda$  is the lobe sharpness.  $\boldsymbol{\xi}$  and  $\frac{1}{\lambda}$  correspond to the mean and variance for the Gaussian function, respectively. The integral of an SG is given by

$$A(\lambda) = \int_{\mathbb{S}^2} G(\boldsymbol{\omega}, \boldsymbol{\xi}, \lambda) d\boldsymbol{\omega} = \frac{2\pi}{\lambda} \left(1 - e^{-2\lambda}\right).$$

In this poster, a normalized SG  $\frac{G(\boldsymbol{\omega}, \boldsymbol{\xi}, \lambda)}{A(\lambda)}$  is used for representing the distribution of reflection lobes.

### 1.1 SG Approximation of reflection lobes

**Diffuse lobes.** For the Lambert bidirectional reflectance distribution function (BRDF)  $\rho_d$ , the diffuse lobe can be approximated with an SG taking energy conservation into account as follows:

$$\rho_d(\mathbf{x}, \boldsymbol{\omega}', \boldsymbol{\omega}) \langle \boldsymbol{\omega}, \mathbf{n} \rangle = R_d \frac{\langle \boldsymbol{\omega}, \mathbf{n} \rangle}{\pi} \approx R_d \frac{G(\boldsymbol{\omega}, \mathbf{n}, \lambda_d)}{A(\lambda_d)}, \quad (1)$$

where  $\boldsymbol{\omega}'$  is the incoming direction,  $\mathbf{n}$  is the surface normal at the position  $\mathbf{x}$ ,  $\langle \boldsymbol{\omega}, \mathbf{n} \rangle = \max(\boldsymbol{\omega} \cdot \mathbf{n}, 0)$ ,  $R_d$  is the diffuse reflectance, and  $\lambda_d \approx 2$  which is obtained by using the least square method.

**Specular lobes.** For the microfacet BRDF  $\rho_s$ , the specular lobe is fitted with a single SG by using Wang et al. [2009]'s analytical approximation. The BRDF is separated into two factors: the normal distribution function (NDF) without a normalization factor  $D(\boldsymbol{\omega}_h)$  and the rest of the factors  $M(\boldsymbol{\omega})$  as follows:

$$\rho_s(\mathbf{x}, \boldsymbol{\omega}', \boldsymbol{\omega}) \langle \boldsymbol{\omega}, \mathbf{n} \rangle = M(\boldsymbol{\omega}) D(\boldsymbol{\omega}_h),$$

where  $\boldsymbol{\omega}_h$  is the half-way vector of  $\boldsymbol{\omega}'$  and  $\boldsymbol{\omega}$ . Bell-shaped NDFs (e.g., Phong [Blinn 1977], Beckmann [1963] and GGX [Walter et al. 2007] NDFs) can be approximated with an SG as

$$D(\boldsymbol{\omega}_h) \approx G(\boldsymbol{\omega}_h, \mathbf{n}, \lambda_h).$$

For Beckmann or GGX NDFs,  $\lambda_h = \frac{2}{\alpha^2}$  where  $\alpha$  is the roughness parameter. Using spherical warping, this can be approximated with a function of  $\boldsymbol{\omega}$  as

$$G(\boldsymbol{\omega}_h, \mathbf{n}, \lambda_h) \approx G(\boldsymbol{\omega}, \boldsymbol{\xi}_s, \lambda_s),$$

where  $\boldsymbol{\xi}_s$  is the reflection vector given by  $\boldsymbol{\xi}_s = 2(\boldsymbol{\omega}' \cdot \mathbf{n})\mathbf{n} - \boldsymbol{\omega}'$ , and  $\lambda_s = \frac{\lambda_h}{4|\boldsymbol{\xi}_s \cdot \mathbf{n}|}$ . Hence, the specular lobe is approximated with the following equation:

$$\rho_s(\mathbf{x}, \boldsymbol{\omega}', \boldsymbol{\omega}) \langle \boldsymbol{\omega}, \mathbf{n} \rangle \approx M(\boldsymbol{\omega}) G(\boldsymbol{\omega}, \boldsymbol{\xi}_s, \lambda_s).$$

Since microfacet BRDFs almost preserve energy for highly glossy surfaces, this poster moreover approximates the specular lobe using a normalized SG as follows:

$$\rho_s(\mathbf{x}, \boldsymbol{\omega}', \boldsymbol{\omega}) \langle \boldsymbol{\omega}, \mathbf{n} \rangle \approx R_s \frac{G(\boldsymbol{\omega}, \boldsymbol{\xi}_s, \lambda_s)}{A(\lambda_s)}, \quad (2)$$

where  $R_s$  is the specular reflectance. Anisotropic SGs (ASGs) [Xu et al. 2013] are also usable in the same manner.

## 2 Virtual Spherical Gaussian Lights

This poster approximates a set of virtual point lights (VPLs) [Keller 1997] with a virtual spherical Gaussian light (VSGL) [Tokuyoshi 2015]. For a VSGL, the total radiant intensity and positional distribution of VPLs are respectively represented using an SG and isotropic Gaussian distribution. This representation can be computed using a simple summation operation.

### 2.1 Radiant intensity

The radiant intensity of the  $i$ th VPL is given as

$$I_i(\boldsymbol{\omega}) = \Phi_i \rho(\mathbf{x}_i, \boldsymbol{\omega}', \boldsymbol{\omega}) \langle \boldsymbol{\omega}, \mathbf{n}_i \rangle,$$

where  $\Phi_i$  is the power of the  $i$ th photon emitted from the light source,  $\boldsymbol{\omega}'$  is the incoming direction of the photon, and  $\mathbf{n}_i$  is the surface normal at the VPL position  $\mathbf{x}_i$ , and  $\rho(\mathbf{x}_i, \boldsymbol{\omega}', \boldsymbol{\omega})$  is the BRDF. This poster first divides this BRDF into diffuse and specular components (i.e.,  $\rho_d$  and  $\rho_s$ ). Then, the total radiant intensity of a set of VPLs is approximated with a single SG for each component by using Toksvig [2005]'s filtering. Therefore, two VSGLs are used for diffuse-specular surfaces. For ease of explanation, this section hereafter describes only a single BRDF component. The total radiant intensity of a set of VPLs  $\mathbb{S}$  is represented as

$$I_v(\boldsymbol{\omega}) = \sum_{i \in \mathbb{S}} I_i(\boldsymbol{\omega}) \approx c_v G(\boldsymbol{\omega}, \boldsymbol{\xi}_v, \lambda_v).$$

To compute  $c_v$ ,  $\boldsymbol{\xi}_v$  and  $\lambda_v$  efficiently, each reflection lobe is approximated using Eq. 1 or Eq. 2 as follows:

$$\begin{aligned} I_v(\boldsymbol{\omega}) &\approx \sum_{i \in \mathbb{S}} \Phi_i R_i \frac{G(\boldsymbol{\omega}, \boldsymbol{\xi}_i, \lambda_i)}{A(\lambda_i)} \\ &= \left( \sum_{i \in \mathbb{S}} \Phi_i R_i \right) \frac{\sum_{i \in \mathbb{S}} \Phi_i R_i \frac{G(\boldsymbol{\omega}, \boldsymbol{\xi}_i, \lambda_i)}{A(\lambda_i)}}{\sum_{i \in \mathbb{S}} \Phi_i R_i}, \end{aligned}$$

where  $R_i$  is the reflectance, and  $\boldsymbol{\xi}_i$  and  $\lambda_i$  are the axis and sharpness of the reflection lobe at the  $i$ th VPL. Then, the weighted average of normalized SGs weighted by  $\Phi_i R_i$  is approximated with a single SG as

$$\frac{\sum_{i \in \mathbb{S}} \Phi_i R_i \frac{G(\boldsymbol{\omega}, \boldsymbol{\xi}_i, \lambda_i)}{A(\lambda_i)}}{\sum_{i \in \mathbb{S}} \Phi_i R_i} \approx \frac{G(\boldsymbol{\omega}, \boldsymbol{\xi}_v, \lambda_v)}{A(\lambda_v)}.$$

Using Toksvig's filtering, the  $i$ th normalized SG is first approximately converted into its averaged direction as  $\bar{\boldsymbol{\xi}}_i = \frac{\lambda_i}{\lambda_i + 1} \boldsymbol{\xi}_i$ . Next, the weighted average of the directions is computed by

$$\bar{\boldsymbol{\xi}}_v = \frac{\sum_{i \in \mathbb{S}} \Phi_i R_i \bar{\boldsymbol{\xi}}_i}{\sum_{i \in \mathbb{S}} \Phi_i R_i}.$$

\*e-mail: tokuyosh@square-enix.com

Finally, the filtered SG is obtained from the weighted average direction as  $\xi_v = \frac{\xi_v}{\|\xi_v\|}$ ,  $\lambda_v = \frac{\|\xi_v\|}{1-\|\xi_v\|}$ . The coefficient  $c_v$  is given by  $c_v = \frac{\sum_{i \in \mathbb{S}} \Phi_i R_i}{A(\lambda_v)}$ .

## 2.2 Positional distribution

In this poster, the positional distribution of VPLs is represented with a single isotropic Gaussian distribution for a VSGL. The weighted mean of VPL positions is computed by

$$\mu_v = \frac{\sum_{i \in \mathbb{S}} \Phi_i R_i \mathbf{x}_i}{\sum_{i \in \mathbb{S}} \Phi_i R_i}$$

The positional variance is also calculated using weighted average as

$$\sigma_v^2 = \frac{\sum_{i \in \mathbb{S}} \Phi_i R_i \|\mathbf{x}_i\|^2}{\sum_{i \in \mathbb{S}} \Phi_i R_i} - \|\mu_v\|^2.$$

Assuming VPLs are distributed on a planar surface, the emitted radiance of a VSGL is represented as follows:

$$L_e(\mathbf{x}, \boldsymbol{\omega}) \approx \frac{I_v(\boldsymbol{\omega})}{2\pi\sigma_v^2 |\boldsymbol{\omega} \cdot \mathbf{n}|} g(\|\mathbf{x} - \mu_v\|, \sigma_v^2), \quad (3)$$

where  $\mathbf{n}$  is the surface normal which will be eliminated in shading (§3.1). Hence, a VSGL is generated by calculating  $\sum_{i \in \mathbb{S}} \Phi_i R_i$ ,  $\sum_{i \in \mathbb{S}} \Phi_i R_i \xi_i$ ,  $\sum_{i \in \mathbb{S}} \Phi_i R_i \mathbf{x}$ , and  $\sum_{i \in \mathbb{S}} \Phi_i R_i \|\mathbf{x}\|^2$ . In this poster, the set of VPLs  $\mathbb{S}$  is all the pixels of a reflective shadow map [Dachsbacher and Stamminger 2005]. Therefore, for each VSGL, the summed values are calculated by using a parallel summation algorithm on the GPU.

## 3 Shading

For each shading point  $\mathbf{x}_p$  with view direction  $\boldsymbol{\omega}_p$ , the reflected radiance is calculated using the rendering equation [Kajiya 1986] defined by

$$L(\mathbf{x}_p, \boldsymbol{\omega}_p) = \int_{\mathbb{S}^2} L_{in}(\mathbf{x}_p, \boldsymbol{\omega}) \rho(\mathbf{x}_p, \boldsymbol{\omega}_p, \boldsymbol{\omega}) \langle \boldsymbol{\omega}, \mathbf{n}_p \rangle d\boldsymbol{\omega}, \quad (4)$$

where  $L_{in}(\mathbf{x}_p, \boldsymbol{\omega})$  is the incoming radiance, and  $\mathbf{n}_p$  is the surface normal at the shading point. This poster approximates the incoming radiance using SGs for the analytical approximation of the rendering integral [Wang et al. 2009; Xu et al. 2013].

### 3.1 Incoming radiance

Using Eq. 3, the approximated incoming radiance is given by

$$\begin{aligned} L_{in}(\mathbf{x}_p, \boldsymbol{\omega}) &= L_e(\mathbf{x}, -\boldsymbol{\omega}) \\ &\approx \frac{I_v(-\boldsymbol{\omega})}{2\pi\sigma_v^2 |\boldsymbol{\omega} \cdot \mathbf{n}|} g(\|\mathbf{x} - \mu_v\|, \sigma_v^2), \end{aligned} \quad (5)$$

where  $\boldsymbol{\omega} = \frac{\mathbf{x} - \mathbf{x}_p}{\|\mathbf{x} - \mathbf{x}_p\|}$ .  $\mathbf{x}$  is assumed to be on the planar surface defined by the normal  $\mathbf{n}$  and position  $\mu_v$ . Here we introduce virtual spherical light (VSL) [Hašan et al. 2009] like approximation to eliminate  $\mathbf{n}$ . In the context of VSLs, a directionally independent shape representation can be used for virtual lights by multiplying  $|\boldsymbol{\omega} \cdot \mathbf{n}|$ . For our case, it is divided by  $|\boldsymbol{\omega} \cdot \mathbf{n}|$ , and thus  $\mathbf{n}$  is eliminated. This is reasonable because the actual surface normal distribution is taken into account by the radiant intensity  $I_v(-\boldsymbol{\omega})$ . Therefore, Eq. 5 is approximated with the following equation:

$$L_{in}(\mathbf{x}_p, \boldsymbol{\omega}) \approx \frac{I_v(-\boldsymbol{\omega})}{2\pi\sigma_v^2} g(\|\mathbf{x}_r - \mu_v\|, \sigma_v^2),$$

where  $\boldsymbol{\omega} = \frac{\mathbf{x}_r - \mathbf{x}_p}{\|\mathbf{x}_r - \mathbf{x}_p\|}$ , and  $\mathbf{x}_r$  is the position on the sphere defined by the center  $\mathbf{x}_p$  and radius  $\|\mu_r - \mathbf{x}_p\|$ . This is derived assuming a

small  $\sigma_v$  or large radius, but it does not produce noticeable artifacts in practice for a large  $\sigma_v$  and small radius. The Gaussian term can be rewritten into an SG as

$$g(\|\mathbf{x}_r - \mu_v\|, \sigma_v^2) = G(\boldsymbol{\omega}, \xi_\mu, \lambda_\sigma), \quad (6)$$

where  $\xi_\mu = \frac{\mu_v - \mathbf{x}_p}{\|\mu_v - \mathbf{x}_p\|}$ , and  $\lambda_\sigma = \frac{\|\mu_v - \mathbf{x}_p\|^2}{\sigma_v^2}$ . This SG represents the spherical region of the VSGL viewed from  $\mathbf{x}_p$ . Our formulation is simpler than Xu et al. [2014]’s virtual area light approximation using an SG. Using Eq. 6, the incoming radiance is approximated with the product of two SGs which yields an SG as follows:

$$\begin{aligned} L_{in}(\mathbf{x}_p, \boldsymbol{\omega}) &\approx \frac{c_v}{2\pi\sigma_v^2} G(\boldsymbol{\omega}, -\xi_v, \lambda_v) G(\boldsymbol{\omega}, \xi_\mu, \lambda_\sigma) \\ &= \boxed{c_{in} G(\boldsymbol{\omega}, \xi_{in}, \lambda_{in})}, \end{aligned} \quad (7)$$

where  $\xi_{in} = \frac{\lambda_\sigma \xi_\mu - \lambda_v \xi_v}{\|\lambda_\sigma \xi_\mu - \lambda_v \xi_v\|}$ ,  $\lambda_{in} = \|\lambda_\sigma \xi_\mu - \lambda_v \xi_v\|$ , and  $c_{in} = \frac{c_v}{2\pi\sigma_v^2} e^{\lambda_{in} - \lambda_v - \lambda_\sigma}$ .

### 3.2 Shading via product integrals of SGs

Since the reflection lobe  $\rho(\mathbf{x}_p, \boldsymbol{\omega}_p, \boldsymbol{\omega}) \langle \boldsymbol{\omega}, \mathbf{n}_p \rangle$  can be approximated using SGs and ASGs, Eq. 4 can be calculated using the analytical product integral.

**Diffuse reflection.** Using Eq. 1 and Eq. 7, the rendering integral of the diffuse component is calculated using the analytical product integral of two SGs. For simplicity, this poster uses Iwasaki et al. [2012]’s approximate product integral as follows:

$$\begin{aligned} L_d(\mathbf{x}_p, \boldsymbol{\omega}_p) &= \int_{\mathbb{S}^2} L_{in}(\mathbf{x}_p, \boldsymbol{\omega}) \rho_d(\mathbf{x}_p, \boldsymbol{\omega}_p, \boldsymbol{\omega}) \langle \boldsymbol{\omega}, \mathbf{n}_p \rangle d\boldsymbol{\omega} \\ &\approx \frac{c_{in} R_d}{A(\lambda_d)} \int_{\mathbb{S}^2} G(\boldsymbol{\omega}, \xi_{in}, \lambda_{in}) G(\boldsymbol{\omega}, \mathbf{n}_p, \lambda_d) d\boldsymbol{\omega} \\ &\approx \frac{2\pi c_{in} R_d G\left(\xi_{in}, \mathbf{n}_p, \frac{\lambda_{in} \lambda_d}{\lambda_{in} + \lambda_d}\right)}{(\lambda_{in} + \lambda_d) A(\lambda_d)}. \end{aligned}$$

In addition, this poster assumes  $A(\lambda_d) \approx \pi$  based on Iwasaki et al.’s approximation. Therefore, diffuse reflection is inexpensively calculated using the following equation:

$$L_d(\mathbf{x}_p, \boldsymbol{\omega}_p) \approx \frac{2c_{in} R_d G\left(\xi_{in}, \mathbf{n}_p, \frac{\lambda_{in} \lambda_d}{\lambda_{in} + \lambda_d}\right)}{\lambda_{in} + \lambda_d}.$$

Unlike previous papers [Xu et al. 2014; Tokuyoshi 2015], this poster represents the cosine factor at the shading point  $\langle \boldsymbol{\omega}, \mathbf{n}_p \rangle$  with  $G(\boldsymbol{\omega}, \mathbf{n}_p, \lambda_d)$  for diffuse surfaces. For a few VSGLs, this SG approximation produces smoother illumination appearance as shown in Fig 1.

**Specular reflection.** While SGs are used for VSGLs, this poster employs an ASG to approximate a specular lobe at a shading point. This is because a specular lobe can be anisotropic even if it is an isotropic BRDF model, especially for shallow grazing angles. For simplicity, ASGs are used only for the first bounce which is more visually important than the second bounce. In addition, the product integral of an ASG and SG [Xu et al. 2013] has a reasonable computation cost. An ASG is defined as

$$\hat{G}(\boldsymbol{\omega}, \xi_x, \xi_y, \xi_z, \eta_x, \eta_y) = \langle \boldsymbol{\omega}, \xi_z \rangle e^{-\eta_x (\boldsymbol{\omega} \cdot \xi_x)^2 - \eta_y (\boldsymbol{\omega} \cdot \xi_y)^2},$$

where  $\xi_x, \xi_y, \xi_z$  are orthonormal vectors, and  $\eta_x, \eta_y$  are the bandwidth parameters. Since a specular lobe is approximated with an

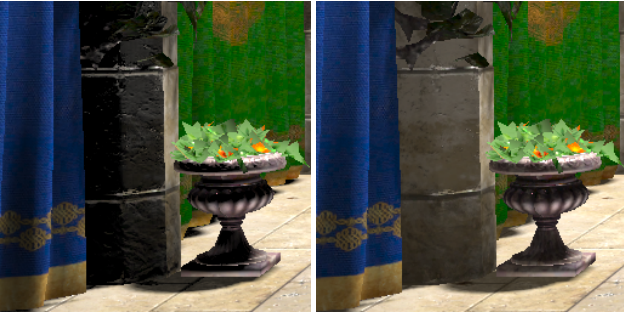


**Figure 1:** Shading using SG approximation for diffuse surfaces. Left: the cosine factor at the shading point is pulled out of the rendering integral [Xu et al. 2014; Tokuyoshi 2015]. Right: SG approximation is used for the cosine factor at the shading point. For a few VSGLs, smoother illumination appearance is produced by approximating the cosine factor with an SG.

ASG as  $\rho_s(\mathbf{x}_p, \boldsymbol{\omega}_p, \boldsymbol{\omega})(\boldsymbol{\omega}, \mathbf{n}_p) \approx M(\boldsymbol{\omega})\dot{G}(\boldsymbol{\omega}, \boldsymbol{\xi}_x, \boldsymbol{\xi}_y, \boldsymbol{\xi}_z, \eta_x, \eta_y)$ , the rendering integral is calculated as

$$\begin{aligned}
 L_s(\mathbf{x}_p, \boldsymbol{\omega}_p) &= \int_{\mathbb{S}^2} L_{in}(\mathbf{x}_p, \boldsymbol{\omega}) \rho_s(\mathbf{x}_p, \boldsymbol{\omega}_p, \boldsymbol{\omega})(\boldsymbol{\omega}, \mathbf{n}_p) d\boldsymbol{\omega} \\
 &\approx c_{in} M(\boldsymbol{\xi}_m) \int_{\mathbb{S}^2} G(\boldsymbol{\omega}, \boldsymbol{\xi}_{in}, \lambda_{in}) \dot{G}(\boldsymbol{\omega}, \boldsymbol{\xi}_x, \boldsymbol{\xi}_y, \boldsymbol{\xi}_z, \eta_x, \eta_y) d\boldsymbol{\omega} \\
 &\approx \frac{\pi c_{in} M(\boldsymbol{\xi}_m) \dot{G}\left(\boldsymbol{\xi}_{in}, \boldsymbol{\xi}_x, \boldsymbol{\xi}_y, \boldsymbol{\xi}_z, \frac{\eta_x \nu}{\eta_x + \nu}, \frac{\eta_y \nu}{\eta_y + \nu}\right)}{\sqrt{(\eta_x + \nu)(\eta_y + \nu)}},
 \end{aligned}$$

where  $\nu = \frac{\lambda_{in}}{2}$ , and  $\boldsymbol{\xi}_m = \frac{\lambda_{in} \boldsymbol{\xi}_{in} + \lambda_s \boldsymbol{\xi}_z}{\|\lambda_{in} \boldsymbol{\xi}_{in} + \lambda_s \boldsymbol{\xi}_z\|}$  is the lobe axis of the integrand.

## References

- BECKMANN, P., AND SPIZZICHINO, A. 1963. *Scattering of Electromagnetic Waves from Rough Surfaces*. MacMillan.
- BLINN, J. F. 1977. Models of light reflection for computer synthesized pictures. *SIGGRAPH Comput. Graph.* 11, 2, 192–198.
- DACHSBACHER, C., AND STAMMINGER, M. 2005. Reflective shadow maps. In *13D'05*, 203–231.
- HAŠAN, M., KŘIVÁNEK, J., WALTER, B., AND BALA, K. 2009. Virtual spherical lights for many-light rendering of glossy scenes. *ACM Trans. Graph.* 28, 5, 143:1–143:6.
- IWASAKI, K., DOBASHI, Y., AND NISHITA, T. 2012. Interactive bi-scale editing of highly glossy materials. *ACM Trans. Graph.* 31, 6, 144:1–144:7.
- KAJIYA, J. T. 1986. The rendering equation. *SIGGRAPH Comput. Graph.* 20, 4, 143–150.
- KELLER, A. 1997. Instant radiosity. In *SIGGRAPH'97*, 49–56.
- TOKSVIG, M. 2005. Mipmapping normal maps. *J. Graph. Tools* 10, 3, 65–71.
- TOKUYOSHI, Y. 2015. Virtual spherical Gaussian lights for real-time glossy indirect illumination. *Comput. Graph. Forum* 34, 7.
- WALTER, B., MARSCHNER, S. R., LI, H., AND TORRANCE, K. E. 2007. Microfacet models for refraction through rough surfaces. In *EGSR'07*, 195–206.

- WANG, J., REN, P., GONG, M., SNYDER, J., AND GUO, B. 2009. All-frequency rendering of dynamic, spatially-varying reflectance. *ACM Trans. Graph.* 28, 5, 133:1–133:10.
- XU, K., SUN, W.-L., DONG, Z., ZHAO, D.-Y., WU, R.-D., AND HU, S.-M. 2013. Anisotropic spherical Gaussians. *ACM Trans. Graph.* 32, 6, 209:1–209:11.
- XU, K., CAO, Y.-P., MA, L.-Q., DONG, Z., WANG, R., AND HU, S.-M. 2014. A practical algorithm for rendering interreflections with all-frequency brdfs. *ACM Trans. Graph.* 33, 1, 10:1–10:16.